SIMULATION OF NANOMETRIC BEND CIRCUITS WITH OPEN-TYPE SURFACE PLASMON GAP WAVEGUIDES BY VOLUME INTEGRAL EQUATION

Kazuo Tanaka, Masahiro Tanaka and Tatsuhiko Sugiyama
Department of Electronics and Computer Engineering of Gifu University, Yanagido 1-1, Japan 501-1193
tanaka@tnk.info.gofu-u.ac.jp

1. Introduction

Nanometric optical integrated circuits are a key optical technology in future applications such as near-field optical (NFO) devices [1, 2], and the surface plasmon polariton (SPPs) on metal surfaces is expected to be employed as a type of nanometric optical wire in such nanoscale integrated optical circuits [3-7]. Although SPPs can travel no more than a few micrometers before extinguishing, such distances are sufficient for nanometer optical integrated circuits. The present authors recently proposed an SPP gap waveguide (SPGW) as a basic element for nanometric optical circuits [8-10]. The waveguiding mechanism of the SPGW is based on the low phase velocity exhibited by SPPs in nanometrically narrow gap regions between two parallel metal substrates compared to that in wide gap regions. SPGWs have been demonstrated to guide, divide, and bend optical waves with acceptable losses in nanometric circuits [8-10]. In previous papers, our group has proposed both closed-type[8, 9] and open-type SPGWs [10], the latter of which provides a more practical structure for E-plane optical circuits. Open-type SPGW (o-SPGW) circuits are easier to fabricate than closed SPGW circuits because the devices can be realized by creating a ditch structure on an open metallic surface. Furthermore, o-SPGW circuits are easier to cool because the open space in the waveguide is connected directly to the surrounding free space, parallel o-SPGWs can be placed adjacently on metallic surfaces, and it is possible to control the optical coupling between waveguides via the field distribution inside each waveguide.

In applying o-SPGWs to practical nanometric optical circuits, the transmission characteristics through the bend structure of the o-SPGW are the most important aspect of their design. In particular, as the o-SPGW is connected directly to open space, radiation loss can become a critical drawback in practical applications. In this paper, the transmission characteristics through the bend structure of an o-SPGW are investigated by three-dimensional simulation using a volume integral equation.

2. Geometry of the problem

The operating wavelength considered in this analysis is $\lambda = 573$ nm, the metal supporting the SPP is assumed to be silver with a relative permittivity of $\varepsilon_1/\varepsilon_0 = -12.4 - j0.85$, and the system is assumed to be

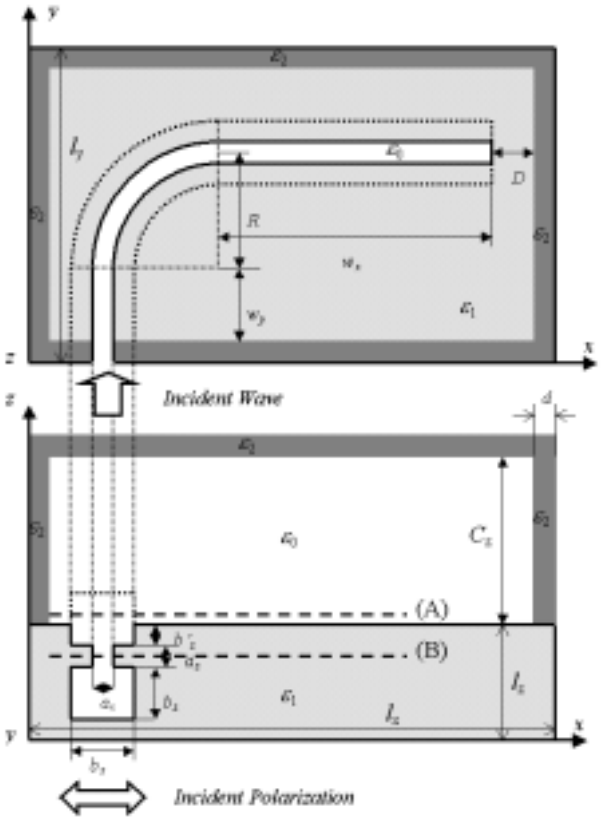

Fig. 1 Schematic of bend-circuit with o-SPGWs.

ISBN: 89-86522-78-0 94460©KEES

governed by an exp(+$j\omega t$) time dependence. A schematic of the E-plane optical circular bend circuits with o-SPGWs considered here is shown in Fig. 1. The silver substrate has dimensions of $l_x \times l_y \times l_z$. The cross-section of the waveguide has an "I" shape, with wide gap region of dimensions $b_x \times b_y$ and narrow gap region of $a_x \times a_y$. The space inside the o-SPGW is connected to the upper free space through the truncated upper wide gap region of the o-SPGW as shown in the figure. The phase velocity of the SPP in the narrow gap region is lower than that in the wide gap region, including free space. It has been shown that optical fields are confined in small gap regions, effectively guiding the fields along the waveguide [8, 10]. The free space region with permittivity of ε_0 above the silver substrate is bounded by five metallic plates with thickness d and relative permittivity of $\varepsilon_2/\varepsilon_0 = -12.4 - j30.91$, as shown in the figure. Without the cover over the substrate, it proved to be difficult to discriminate the guided field in the o-SPGWs from the field excited by the diffracted incident wave. The void space inside the o-SPGWs is assumed to be free space with permittivity of ε_0 in this analysis.

The E-plane bend circuit using o-SPGWs consists of a short straight section with length w_y, a circular bend section with average radius R, and a long straight section with length w_x, as shown in Fig. 1. A plane wave is assumed to be incident on the short straight section from the negative y direction through the I-shaped aperture formed in the substrate and cover. In order to excite the SPP inside the waveguide, the incident electric field must be oriented in the x direction. The excited SPP in the short straight section is transmitted to the long straight section through the circular bend-section. The exits of the long straight sections of the o-SPGWs are closed in order to prevent the introduction of a diffracted incident wave from the ends of the waveguide. The long straight section is made sufficiently long to ensure that the end of the waveguide is connected to the matched terminal, that is, to ensure no reflection from the end of the waveguide. To ensure that the field in the short straight section is the guided mode of the o-SPGW, the incident vector is set to be rotated by $\pi/4$ with respect to the positive z axis to achieve oblique incidence to the entrance aperture.

3. Volume integral equation

The scattering problem for the metallic structure shown in Fig. 1 is solved using a volume integral equation, as given by [11-13]

$$\boldsymbol{E}^i(\boldsymbol{x}) = \boldsymbol{D}(\boldsymbol{x})/\varepsilon_r(\boldsymbol{x}) - (k_0^2 + \nabla\nabla\bullet)\boldsymbol{A}(\boldsymbol{x}) \quad (1)$$

where $k_0 = \omega/c$ (c is light velocity in free space), $\boldsymbol{D}(\boldsymbol{x})$ is the total electric flux, $\boldsymbol{E}^i(\boldsymbol{x})$ is the incident electric field, and $\boldsymbol{A}(\boldsymbol{x})$ is the vector potential, which is expressed by the following volume integral.

$$\boldsymbol{A}(\boldsymbol{x}) = (1/\varepsilon_0)\iiint_V \{[\varepsilon_r(\boldsymbol{x}') - \varepsilon_0]/\varepsilon_r(\boldsymbol{x}')\} G(\boldsymbol{x}|\boldsymbol{x}')\boldsymbol{D}(\boldsymbol{x}')dv' \quad (2)$$

Here, $G(\mathbf{x}|\mathbf{x}')$ is a free-space Green's function given by

$$G(\boldsymbol{x}|\boldsymbol{x}') = \exp(-jk_0|\boldsymbol{x} - \boldsymbol{x}'|)/(4\pi|\boldsymbol{x} - \boldsymbol{x}'|) \quad (3)$$

The volume integral region V in Eq. (2) represents the entire space, and $\varepsilon_r(\mathbf{x})$ represents the distribution of permittivity, where $\varepsilon_r(\mathbf{x}) = \varepsilon_0\varepsilon_1$ in silver and $\varepsilon_r(\mathbf{x}) = \varepsilon_0$ in the void space of the circuits. Since the region in which $[\varepsilon_r(\mathbf{x}') - \varepsilon_0]$ is nonzero is finite and the integral region V has finite volume, it is possible to solve Eq. (1) numerically by the well-established method of moments. To obtain the solution, entire region of the circuit is divided into small discretized cubes of size $\delta \times \delta \times \delta$, and Eq. (1) is discretized by the method of moments using roof-top functions as basis and testing functions. The resultant large system of linear equations is then solved by iteration using the generalized minimized residual method (GMRES) and fast Fourier transform (FFT) [14].

3. Numerical simulations

The parameters used in the model bend circuit were as follows. Circuit size: $k_0 l_x = 50.0$ (4560 nm), $k_0 l_y = 12.5$ (1140 nm), $k_0 l_z = 2.8$ (255 nm), and $k_0 D = 1.0$ (91 nm). Cross-section of o-SPGWs: $k_0 a_x = k_0 a_z = 0.4$ (36 nm), $k_0 b_x = 0.8$ (73 nm), $k_0 b_z = 1.4$ (128 nm). Cover: $k_0 C_z = 9.2$ (839 nm) and $k_0 d = 1.0$ (91 nm). Discretized cube: $k_0\delta = 0.1$ (9 nm). The sizes in parentheses indicate approximate practical sizes for $\lambda = 573$ nm. The overall dimensions of the optical circuits with the cover are approximately $8.0\lambda \times 2.0\lambda \times 1.9\lambda$. These values are

not optimized. In order to position the region of strong optical intensity as near the surface of the

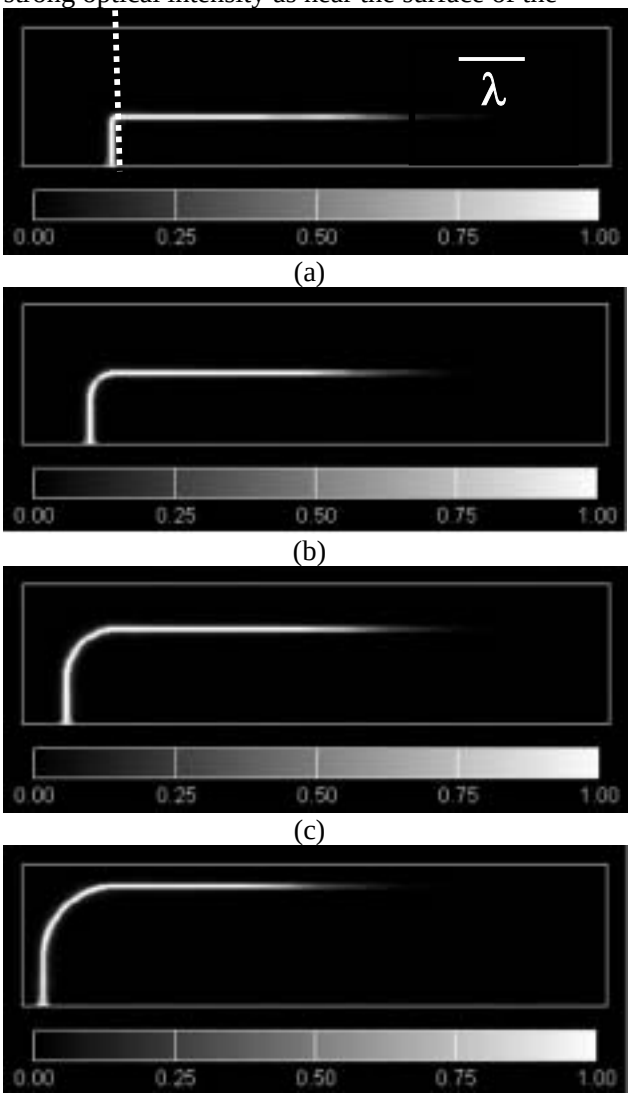

(a) (b) (c) (d)

Fig. 2. Distributions of optical intensity on the plane (B) in Fig. 1 for average radii k_0R of (a) 0.4, (b) 2.2, (c) 4.2, and (d) 6.2. The intensity scale is normalized by the incident intensity. The white outline represents the boundary of the silver substrate.

circuit as possible, k_0b_z' shown in Fig. 1 was set to 0 in this treatment.

The electric field distribution of the circuits shown can be obtained by solving Eq. (1) numerically. The distributions of optical intensity (i.e., $|\boldsymbol{E}|^2$) for the case of a unit intensity incident field (i.e., $|\boldsymbol{E}^i|^2 = 1$)

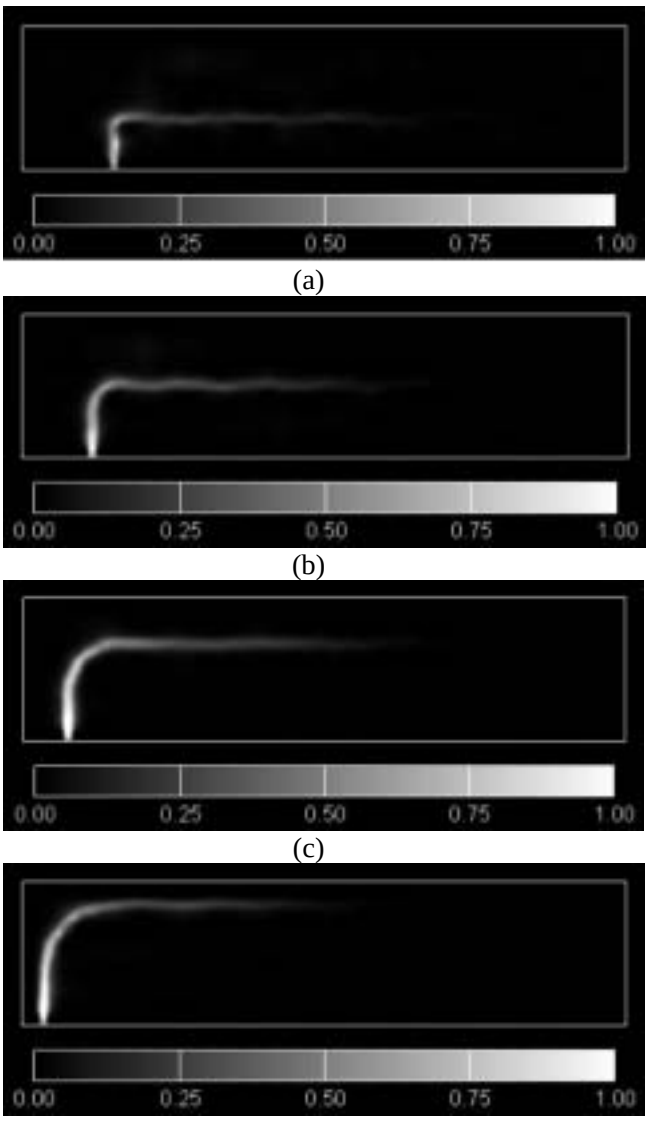

(a) (b) (c) (d)

Fig. 3. Distribution of optical intensity on the plane (A) in Fig. 1 for average radii k_0R of (a) 0.4, (b) 2.2, (c) 4.2, and (d) 6.2. The intensity scale is normalized by the incident intensity. The white outline represents the boundary of the silver substrate.

are shown in Fig. 2 on a plane parallel to the *x*-*y* plane indicated by (B) in Fig. 1 for $k_0R = 0.4$ (36 nm), 2.2 (201 nm), 4.2 (383 nm), and 6.2 (565 nm). Enhanced optical intensities occur in the narrow gap region of the o-SPGWs, demonstrating that the optical waves are confined and guided along the bend circuit. The radiation fields around these bend circuits were determined based on the optical intensity on the plane parallel to the *x*-*y* plane in the

free-space region indicated by (A) in Fig. 1, as shown in Fig. 3. The distance h between this plane and the surface of the circuit is given by $k_0h = 0.05$ (5 nm). The free-space region surrounded by the metallic cover above the substrate is sufficiently large to admit radiation from the bend-section. However, no optical intensity distribution that could be related to the radiation field was observed in the free-space region inside the cover. The distribution of optical intensity on the plane parallel to the y-z plane near the bend section and short straight section is shown in Fig. 4. Figure 4 represents the result on the planes indicated by the broken lines in Fig. 2(a) of k_0R=0.4. This result also shows that the optical field is confined in the narrow gap region and indicate the absence of radiation fields. The results in Figs. 2–4 are independent of the height of the cover C_z when sufficiently large.

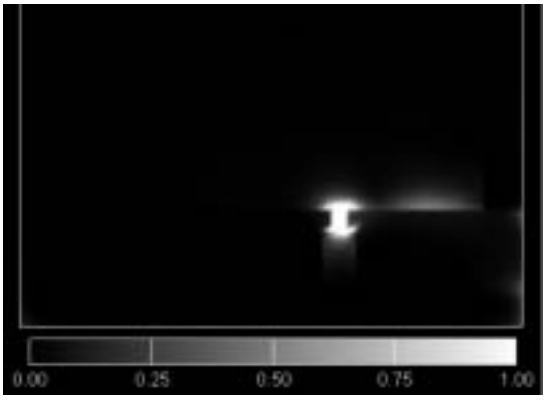

Fig. 4. Distribution of optical intensity on the planes indicated by broken lines in Fig. 2(a). The white outline represents the boundary of the silver substrate and the cover. The intensity scale is normalized by the incident intensity.

4. Conclusions

The computer simulation of transmission characteristics of a nanometric bend circuit constructed using open-type SPP gap-waveguides were investigated by three-dimensional numerical simulation. Although the o-SPGWs are connected to free space, the radiation loss was found to be negligible compared to the propagation and insertion losses. The simulations also showed that a bend radius smaller than the operating wavelength can be used in practical optical circuits.

ACKNOWLEDGEMENT

This study was financially supported by a 2004 Grant-in-Aid for Scientific Research from the Ministry of Education, Science, Sports and Culture of Japan..

References

1. D. W. Pohl and D. Courjon ed., *Near Field Optics*, Kluwer Academic (1993).
2. M. Ohtsu and H. Hori, *Near-Field Nano-Optics*, Kluwer Academic/Plenum Publishers, New York (1999).
3. J. Takahara, S. Yamagishi, H. Taki, A. Morimoto and T. Kobayashi, Opt. Lett., **22** 4765(1997).
4. S. A. Maier, M. L. Brongersma, P. G. Kik, S. Meltzer, A. A. G. Requicha, H. A. Atwater, Adv. Mat. **13**, 1501(2001).
5. T. Yatsui, M. Kourogi, and M. Ohtsu, Appl. Phys. Lett. **79**, 4583 (2001).
6. T. Goto, Y. Katagiri, H. Fukuda, H. Shinojima, Y. Nakano, I. Kobayashi, Y. Mitsuoka, Appl. Phys. Lett. **84**, 852(2004).
7. H. Ditlbacher, J. R. Krenn, G. Schider, A. Leitner, F. R. Aussenegg, Appl. Phys. Lett. **81**, 1753(2002).
8. K. Tanaka and M. Tanaka, Appl. Phys. Lett. **82**, 1158(2003).
9. K. Tanaka, M. Tanaka and T.Sugiyama, Optics Exp. 13, 256(2005).
10. K. Tanaka and M. Tanaka, Jpn. J. Appl. Phys. **42**, L585(2003).
11. E. K. Miller, L. Medgyesi-Mitschnag and E. H. Newsman ed.: *Computational Electromagnetics Frequency-Domain Method of Moments*, Institute of Electrical and Electronics Engineers, Inc. (1992).
12. J. H. Wang, *Generalized Moment Method in Electromagnetics: Formulation and Computer Solution of Integral Equations*, John Wiley & Sons, Inc. New York (1991).
13. P. Zwamborn and P. M. van den Berg, IEEE Trans on MTT, **MTT-40**, 1757(1992).
14. R. Barrett, M. Berry, T. F. Chan, J. Demmel, J. Donato, J. Dongarra, V. Eijkhout, R. Pozo, C. Romine and H. van der Vorst, *Templates for the Solution of Linear Systems: Building Blocks for Iterative Methods*, Society for Industrial and Applied Mathematics (1994).